Chapter 6

Deep Structure of Supergranular Flows[1]

6.1 Previous Observations

Granulation, observed at the solar photosphere, with a typical size of 1 Mm and lifetime of 10 minutes, is believed to be a solar convective structure. Supergranulation was first observed in 1950s (Hart, 1954), and was later also associated as convective cells (Leighton, Noyes, & Simon, 1962), although this interpretation is still at dispute.

Supergranulation is characterized by its horizontal divergent flows, observed either by direct Doppler velocities when the supergranulation is away from the disk center (e.g., Hart, 1954; Leighton, Noyes, & Simon, 1962), or by tracking the advection of magnetic elements or granules (e.g., Simon, 1967; November & Simon, 1988). Its typical scale is 32 Mm and typical lifetime is 20 hours, and the horizontal outflows have a speed of the order of 500 m/s. The supergranular flow pattern appears cellular, diverging from center outward and terminating at boundaries outlined by strong photospheric magnetic fields that are corresponding to chromospheric magnetic networks. Measurements of downflows at supergranular boundaries are often complicated by the presence of magnetic elements, and this makes the Doppler velocity very difficult to

[1]Part of this chapter was published in *Proceeding of SOHO 12/GONG+ 2002 Workshop* (Zhao & Kosovichev, 2003a)

disentangle from effect of the magnetic field by use of spectrum. Nevertheless, downward flows with speed of tens to hundreds of meters per second were reported (e.g., Frazier, 1970; Wang, 1989), and the downward flows often concentrated in the small regions where magnetic field appeared. If the downward flows at the supergranular boundaries are still detectable, the vertical velocity at the supergranular centers are hardly measurable. No reliable measurements have so far been reported from spectral analyses.

The other interesting and well-known characteristic of supergranules is its super-rotation rate. By tracking the supergranular pattern at the solar surface, it was found that supergranules rotate much faster than the solar plasma, and also faster than the surface magnetic features (Duvall, 1980; Snodgrass & Ulrich, 1990). This remained a puzzle for two decades. Recently, Gizon, Duvall, & Schou (2003) and Schou (2003) found the wave-like features of supergranulation which may help to explain the super-rotation rate. The rotational speed of supergranular patterns may be an addition of the real rotational speed of supergranulation and the wave propagation speed. The real rotation speed of supergranules derived by subtracting the wave propagation speed from the supergranular patterns speed is similar to the speed of magnetic features, and this was then interpreted by the authors as that supergranules may have a common origin with solar surface magnetic features.

In this chapter, we will attempt to obtain the subsurface flow fields by doing inversions on time-distance measurements of supergranules. And we also try to determine the depth of supergranules by correlating the divergent flows with the return flows at some depths.

6.2 "Cross-talk" Effects in Inversion

Strong "cross-talk" effects will affect our inversions for time-distance measurements of supergranular flows. This is because, at the center the supergranules, strong horizontal divergence can accelerate the outgoing waves and decelerate the ingoing waves in the same way as the downward flows do; while at the boundary of supergranules,

strong horizontal convergence can accelerate the ingoing waves and decelerate outgoing waves in the same way as the upward flows do. On the other hand, the vertical flow speed of plasma at the center of supergranules is often one order smaller than the horizontal velocity. So, in some cases, the horizontal divergence may be inverted as downward flows, which we should avoid.

Therefore, many artificial experiments were designed to test the ability of our inversion code to solve the "cross-talk" effects. Figure 6.1 shows a very interesting example which reminds us to be very cautious in doing inversions. The upper panel of Figure 6.1 shows an artificial model of flows having a strong horizontal divergence but very weak vertical flow speed, which may perhaps simulate the flow structures of supergranules. The lower two panels of Figure 6.1 show the inversion results by LSQR algorithm with 5 and 100 iteration steps. Interestingly, but not surprisingly, results with 5 iteration steps gave downward flows at the center of the divergent regions, which is not the case in the original data. However, it seems that the results with 100 iteration steps can recover perfectly the shallow flow fields. This numerical experiment shows us that "cross-talk" can result in incorrect vertical velocity in inversions for a small number of iteration steps.

As a summary after various artificial models experiments, it was found that for different flow structures, "cross-talk" effects can be significant or not. However, after a sufficiently large number of iterations, the vertical flows can still be nearly or totally recovered for noise-free data. But, for the case of real data, since noises are unavoidable, it is usually impractical to have a large number of iterations because noises can be easily magnified and transported to other locations. The optimal number of iterations selected in practice is larger than 5, but less than 20.

6.3 Inversion for Supergranules

6.3.1 Supergranular Flows

A set of 512-minute high-resolution MDI data was used for time-distance analysis to derive the flow fields of supergranules. Measurements and inversions were performed

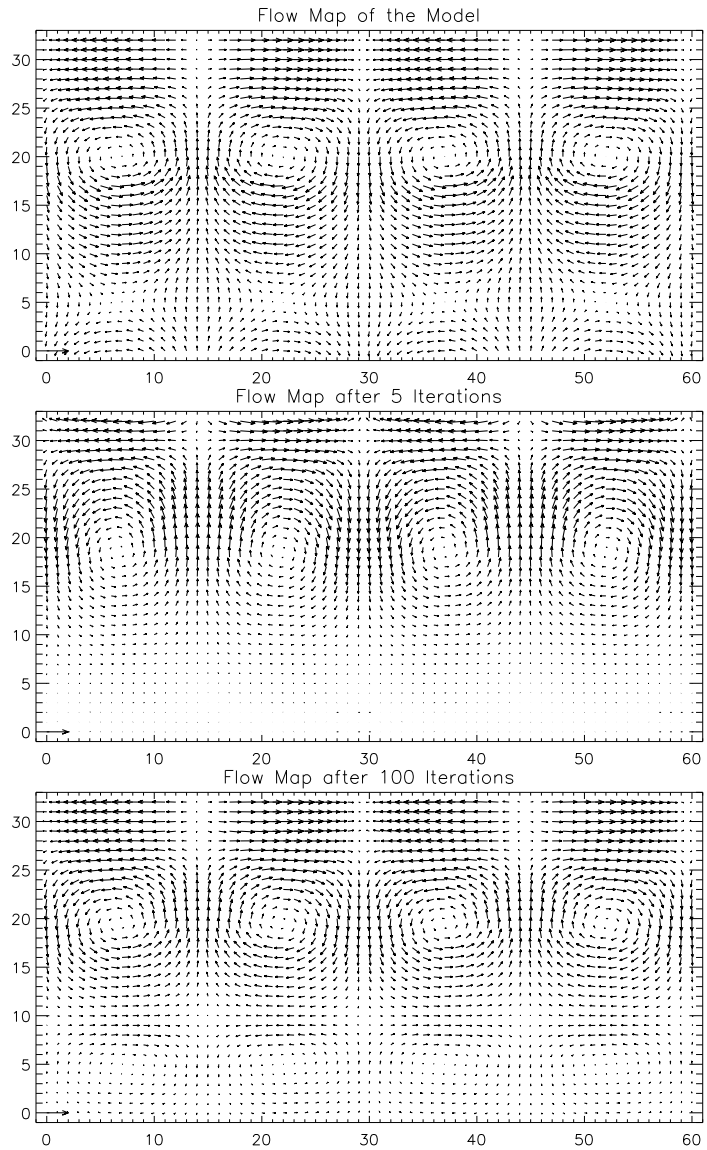

Figure 6.1: An example of inversion tests over artificial models. The upper panel shows an artificial flow field in a vertical cut. The two lower panels show the inversion results of noise-free travel times after 5 and 100 iterations.

as described in Chapter 2. Due to the perhaps confused vertical flow directions as demonstrated in the last section, we only present the horizontal flow fields in the following.

Figure 6.2 shows one large supergranule with very strong divergence picked from

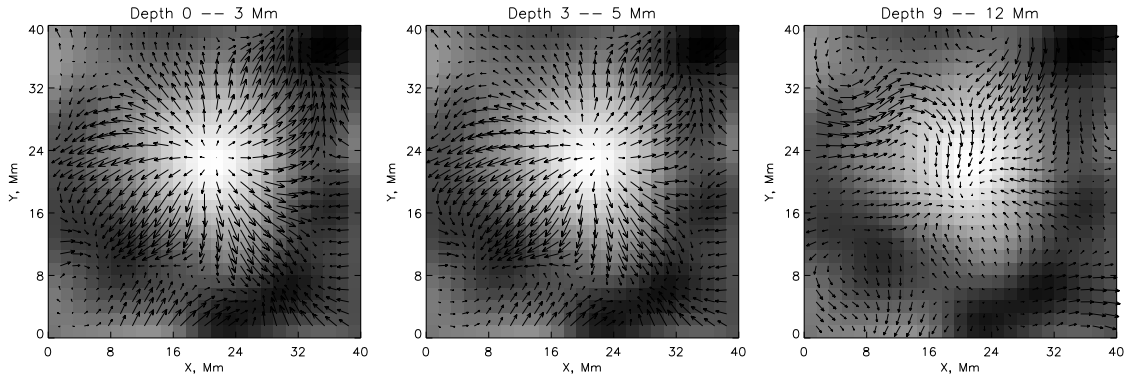

Figure 6.2: Horizontal flows of a supergranule from inversion results of the MDI data. The background image of each graph is the divergence of flows near the solar surface to indicate the location of the supergranule, with white as divergence and dark as convergence. The longest arrow in each panel represents approximately 500 m/s.

the studied region, with the center of the supergranule at approximately latitude 6° in North hemisphere and when it is passing the central meridian. The horizontal flow maps at three different depth intervals are presented. Outflows from the central supergranular region can be seen at the depths from the surface to about 5 Mm. However, at the depth of 9 – 12 Mm, convergent flows are found with smaller speed, though not toward exactly the center of the supergranule observed at the surface.

It should also be pointed out that the return convergent flows are not seen for all the supergranules. Except some large supergranules with strong divergence, most other supergranules do not show returning flows in deeper layers. Random flows, which may be caused by noise propagation or systematic errors, dominate the flow structures below the depth of 6 Mm or so for such supergranules.

6.3.2 Depth of Supergranules

Although the vertical flows have not been reliably derived from our inversions, the convergent flows found at depth of ∼10 Mm may suggest that the supergranules are cellular convective structures. If this is true, we may estimate the depth of supergranules by the following means. In a quiet solar region of approximately 200 Mm × 200 Mm, which includes about 30 supergranules, we calculate the divergence

$\nabla \cdot \mathbf{v}_h = \partial v_x/\partial x + \partial v_y/\partial x$ from the inverted horizontal velocities at different depth intervals. Then we compute the correlation coefficients of the divergence map at each depth with the divergence map of the first layer.

Figure 6.3 shows the results of correlation coefficients as a function of depth. The coefficient drops from 1.0 to 0.0 with the increase of depth, and continues to drop to the negative until -0.5. This may indicate that the divergent flow structures may extend from the surface to around 6 Mm, and then are replaced by the returning convergent flows, which extends to a depth of around 14 Mm. From this plot of correlation coefficients, we may estimate that the depth of supergranules are approximately 14 Mm.

Previously, Duvall (1998) estimated the depth of supergranules to be around 8 Mm by calculating the correlation coefficients between horizontal components of velocities

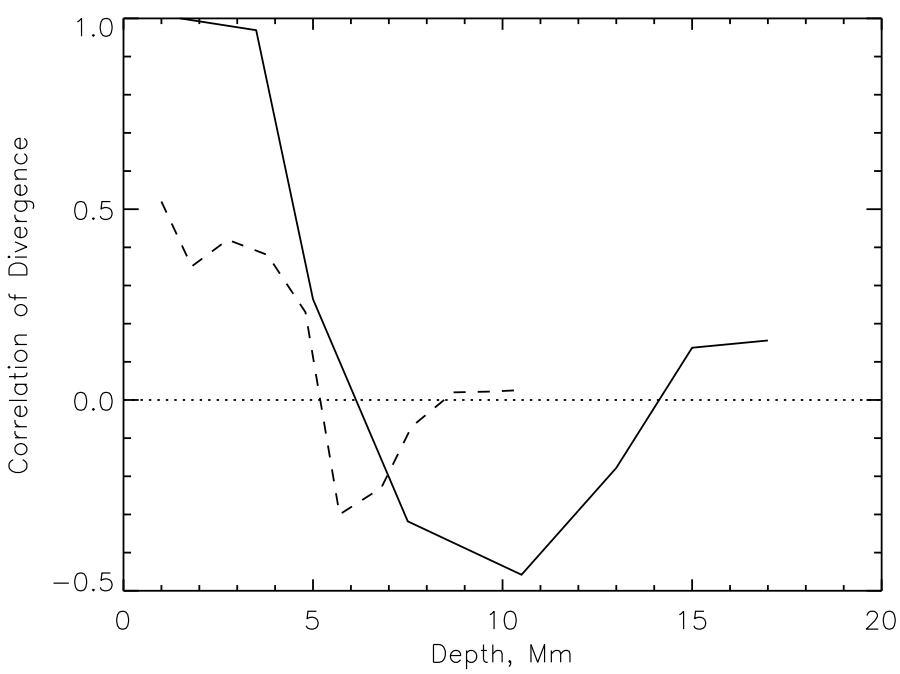

Figure 6.3: Correlation coefficients (*solid curve*) between the divergence maps at each different depth and the divergence map of the top layer (from this study). The dashed curve shows the correlation between horizontal velocities at different depths with the top layer (from Duvall, 1998). The dotted line indicates the 0 line.

at different depths and the velocities at the surface (also shown in Figure 6.3). But that work (Duvall, 1998) did not exclude the f-modes when doing time-distance measurements, which probably cause the shallowness of the depth result. The result presented here has significantly extended the estimated depth of supergranules, which may be closer to what some researchers expected (Hathaway et al., 2000).

6.4 Discussion and Summary

Various artificial data experiments have shown us how the inversion codes can provide us inaccurate and even opposite results. This cautions us the necessity of designing various artificial experiments before doing inversions on real observations, and suggests care when interpreting inversion results.

Due to the nature of the weak vertical supergranular flow speed, we failed to derive reliable vertical flows like previous studies based on analyzing spectral lines. The issue is that the number of inversion iterations is limited by noise propagation and magnification. However, if we have more knowledge of time-distance measurement errors and are able to incorporate the error covariance matrix into the inversion code, we may increase the number of inversion iterations and prevent the fast propagation and magnification of measurement errors. On the other hand, some constraints may also be provided to the inversion code in order to have reliable results with relatively small number of iterations. Such constraints may include the conservation of mass and the minimization of kinetic energy. However, we have not found an effective way to incorporate such constraints into the LSQR inversion code.

In this study, we have found return converging flows of supergranules at a depth of approximately 10 Mm. This may indicate the flow structures of supergranules are cellular, like most researchers expected. Base on this assumption, we estimated the depth of supergranules to be around 14 Mm, which is similar to the depth as some researchers expected. Braun & Lindsey (2003) computed the ratio of velocities at different depths that were derived from acoustic holography technique, and found a similar curve as shown in Figure 6.3, from which they suggested supergranules have a convective structure.

The computations presented in this chapter can be extended to a few Carrington rotations which were taken during the MDI Dynamic Campaign periods. By such computations, solar rotational speed and meridional flows can be inferred; and latitudinal vorticity distribution can also be derived. These results will be presented and discussed in the next chapter.